ISSN 0023-1584, Kinetics and Catalysis, 2006, Vol. 47, No. 1, pp. 98–105. © MAIK "Nauka/Interperiodica" (Russia), 2006.
Original Russian Text © V.V. Sinel'nikov, N.N. Tolkachev, S.S. Goryashchenko, N.S. Telegina, A.Yu. Stakheev, 2006, published in Kinetika i Kataliz, 2006, Vol. 47, No. 1, pp. 103–110.

Propane Oxidation with Chemically Bound Oxygen on $Pt/TiO_2/Al_2O_3$ and $Pt/CeO_2/Al_2O_3$ Catalysts

V. V. Sinel'nikov, N. N. Tolkachev, S. S. Goryashchenko, N. S. Telegina, and A. Yu. Stakheev

Zelinskii Institute of Organic Chemistry, Russian Academy of Sciences, Moscow, 117334 Russia

Received March 15, 2005

Abstract—Possible mechanisms are suggested for propane oxidation on $Pt/TiO_2/Al_2O_3$ and $Pt/CeO_2/Al_2O_3$ catalysts in the cyclic reactant supply mode. As compared to the steady-state process, the process conducted as catalyst oxidation–reduction cycles results in a very different product composition: it is more selective toward partial oxidation products and yields much smaller amounts of complete oxidation products. It is established by isothermal and temperature-programmed oxygen desorption that, under the reaction conditions examined, the oxygen desorbed from the catalyst surface into the gas phase makes a negligible contribution to propane oxidation. It is proved by XPS that propane oxidation is due to the chemically bound oxygen of the catalyst. The hypothetical mechanism of the process includes propane activation on Pt followed by the transfer of the activated species to the oxygen-storing component (TiO_2 or CeO_2), where the intermediates are oxidized by chemically bound oxygen.

DOI: 10.1134/S0023158406010150

INTRODUCTION

The oxidative conversion of natural lower paraffins (C_1–C_3) into valuable products is a challenging problem of heterogeneous catalysis. Solving this problem is expected to result in comparatively cheap and environmentally friendly processes. The selectivity of oxidative conversion is limited by oxygen present in the gas phase under catalytic conditions. The decrease in the selectivity of the process arises from the further homogeneous and heterogeneous oxidation of the desired products to CO_2 and H_2O. Therefore, it is of considerable interest not only to develop more selective and active catalysts but also to conduct catalytic oxidation in a cyclic (periodic) mode in which portions of the reactants are alternately admitted to the catalyst [1]. In this technology, the hydrocarbons are oxidized in the absence of gas-phase O_2, utilizing oxygen stored by the catalyst. This approach allows the selectivity of some processes to be markedly increased [2].

The periodic technology is promising for methane conversion into synthesis gas, the oxidative condensation of methane to heavier hydrocarbons [3], the oxidative dehydrogenation of ethane to ethylene and of propane to propylene [4], and the oxidation of butane to maleic anhydride [5].

However, the cyclic technology entails a decrease in the efficiency of the process, because classical partial oxidation catalysts are incapable of storing considerable amounts of oxygen and show low activities [6]. The first obstacle can be overcome by introducing a component with a high oxygen storage capacity into the catalyst [7]. An increase in the reaction rate can be achieved by adding more active components such as noble metals.

Here, we report a comparative study of reaction mechanisms for propane oxidation on $Pt/TiO_2/Al_2O_3$ and $Pt/CeO_2/Al_2O_3$ catalysts in such a way that portions of C_3H_8 and O_2 are alternately fed into the reactor. CeO_2 and TiO_2 are introduced in these catalytic systems for the purpose of increasing the oxygen storage capacity. CeO_2 is a classical oxygen-storing oxide [8], and we have demonstrated that TiO_2 also has a high oxygen storage capacity [7]. Platinum is introduced to increase the reaction rate. A similar approach was described in earlier papers [9, 10]. The catalytic properties of the supported systems TiO_2/Al_2O_3, $Pt/TiO_2/Al_2O_3$, CeO_2/Al_2O_3, and $Pt/CeO_2/Al_2O_3$, are compared with those of the mechanical mixtures of their components ($Pt/Al_2O_3 + TiO_2/Al_2O_3$ and $Pt/Al_2O_3 + CeO_2/Al_2O_3$). The catalytic systems are characterized by isothermal O_2 desorption (O_2 ID), temperature-programmed O_2 desorption (O_2 TPD), and XPS.

EXPERIMENTAL

Catalyst Preparation

A catalyst of composition $10\%CeO_2/Al_2O_3$ was prepared by impregnating Al_2O_3 with an aqueous solution of $Ce(NO_3)_3$.

Catalysts of composition $1\%Pt/10\%CeO_2/Al_2O_3$ were prepared by the incipient-wetness impregnation of alumina (S_{BET} = 184 m^2/g) with an aqueous solution containing $Ce(NO_3)_3$ and H_2PtCl_6.

$1\%Pt/10\%TiO_2/Al_2O_3$ catalysts were prepared in two steps:

(1) Al_2O_3 was impregnated with a $C_{12}H_{28}O_4Ti$ solution in isopropyl alcohol. The resulting solid was dried and calcined in air at 600°C for 2 h.

(2) The resulting TiO_2/Al_2O_3 material was impregnated with an aqueous solution of H_2PtCl_6.

The solids thus obtained were dried in air at room temperature and then calcined in air at 600°C for 2 h. The calcination temperature was raised at a rate of 0.5 K/min. The calcination products were reduced in flowing H_2 at 400°C for 2 h, raising the temperature at a rate of 2 K/min.

Study of Catalytic Properties

Catalytic properties were studied using a flow catalytic reactor (Fig. 1) operating in a cyclic mode. An oxidation–reduction cycle consisted of the following steps:

(1) The catalyst was treated with flowing air for 60 s at a prescribed temperature. Oxygen accumulation in the catalyst took place at this stage.

(2) The catalyst was treated with flowing N_2 to remove the oxygen from the gas phase and the weakly bound oxygen from the catalyst surface.

(3) A 10-s pulse of C_3H_8 (5000 ppm)–N_2 gas mixture was fed into the reactor.

(4) A 10-s pulse of N_2 was fed into the reactor to remove the products that resulted from the previous step of the process.

Steps 3 and 4 were repeated several times.

The feed composition was varied by adding air, propane, or nitrogen to the main nitrogen flow, using electromagnetic valves (*1–3*) (Fig. 1). In all process steps, the VHSV was 40 000 h^{-1} and the catalyst bed temperature was 400°C.

A catalyst sample of volume 0.5 cm^3 was placed in a quartz reactor with an inner diameter of 7 mm. The outlet CO and CO_2 concentrations were determined using gas analyzers with IR detectors (*6*, *7*). The total amount of hydrocarbons (ΣC_xH_y) in the gas mixture was determined using a gas analyzer with a flame-ionization detector (*8*). The composition of the hydrocarbon mixture was precisely determined by gas chromatography. The sampled gas was separated into CH_4, C_2H_4, C_2H_6, C_3H_6, and C_3H_8 using a 2-m-long Porapak Q column at 60°C. In order to average out the composition of the product mixture and smooth away the concentration jumps arising from feed switching, the samples were taken from an averaging vessel (*9*) (Fig. 1). The residence time of the flowing gas in this vessel was 15 min.

Figure 2 illustrates the typical response of the CO, CO_2, and C_xH_y gas analyzers to the introduction of propane and air pulses into the reactor packed with an air-pretreated catalyst (step 1).

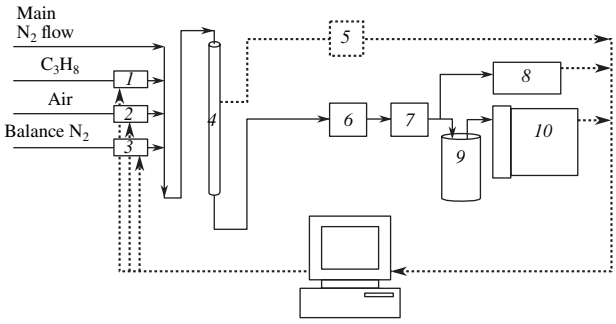

Fig. 1. Propane oxidation setup: (*1–3*) computer-controlled electromagnetic valves, (*4*) reactor, (*5*) temperature controller, (*6*) CO analyzer, (*7*) CO_2 analyzer, (*8*) total hydrocarbon analyzer, (*9*) averaging vessel, and (*10*) chromatograph.

The calculation of main process parameters was based on carbon balance, so all of the data presented here are per one carbon atom (C_1).

The total amount of hydrocarbons in the gas mixture ($n\Sigma C_xH_y$) and the amounts carbon monoxide and dioxide resulting from propane oxidation (nCO and nCO_2, respectively) were derived from peak area data (Fig. 2). The amount of condensation products deposited on the catalyst surface (nC) was determined from the amounts of CO and CO_2 resulting from the oxidative treatment of the catalyst. The average concentrations of individual hydrocarbons were determined chromatographically. The amount of a hydrocarbon in the mixture leaving the reactor was calculated by the formula

$$nC_xH_y = n\Sigma C_xH_y[C_xH_y],$$

where $n\Sigma C_xH_y$ is the total amount of hydrocarbons in the gas mixture and $[C_xH_y]$ is the average concentration of the hydrocarbon.

It is clear from Fig. 2 that, for example, after eight pulses, the outlet concentrations of carbon oxides vary negligibly. For this reason, the time distribution of reaction products was measured for a cycle including ten propane pulses.

O_2 ID and O_2 TPD

The O_2 ID procedure was as follows:

(1) The catalyst was treated with flowing air at 400°C for 1 h.

(2) The catalyst was cooled to 30°C in flowing air.

(3) The catalyst was heated to 400°C in flowing argon.

(4) O_2 concentration was measured in the flowing argon at 400°C.

The volume of the catalyst sample was 0.5 cm^3, and the air and argon flow rates were 100 ml/min. The purpose of these O_2 ID measurements was to determine the amount of oxygen desorbed at 400°C and the desorption time.

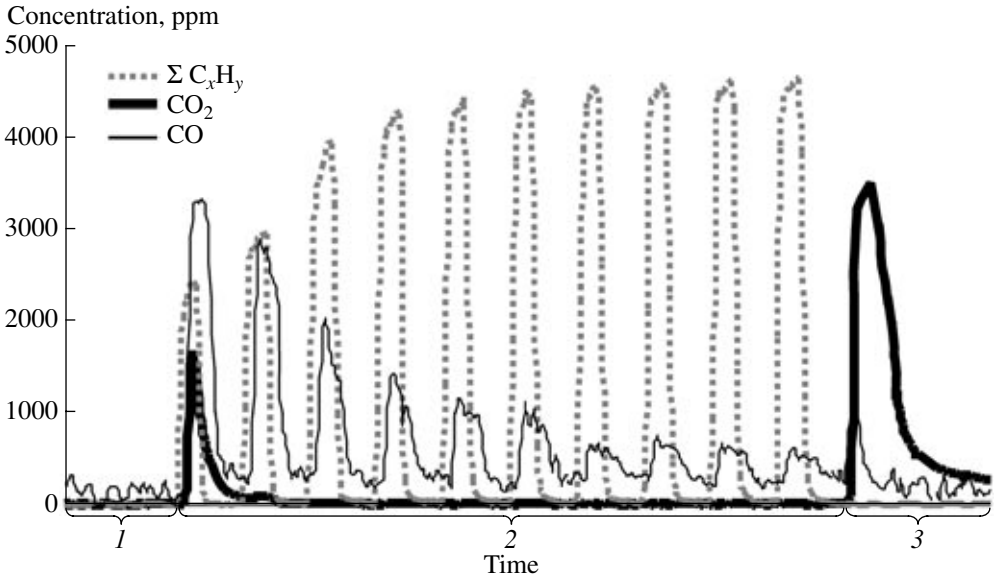

Fig. 2. Hydrocarbon, CO, and CO_2 concentrations as a function of time (the number of pulses): (*1*, *3*) catalyst oxidation stages and (*2*) propane oxidation stage.

The O_2 TPD procedure was as follows:

(1) The catalyst was treated with flowing air at 400°C for 1 h.

(2) The catalyst was cooled to 30°C in flowing air.

(3) The catalyst was heated to 800°C at a linear rate of 10 K/min.

The volume of the catalyst sample was 0.5 cm^3, and the air and argon flow rates were 100 ml/min. The purpose of these O_2 TPD measurements was to determine the amount of oxygen desorbable from the catalyst and the desorption time.

The amount of desorbed oxygen was determined by integrating the oxygen concentration as a function of time.

Oxygen concentration was measured with an NIFRIT gas analyzer (Angarskii OKBA, Russia), equipped with a coulometric detector.

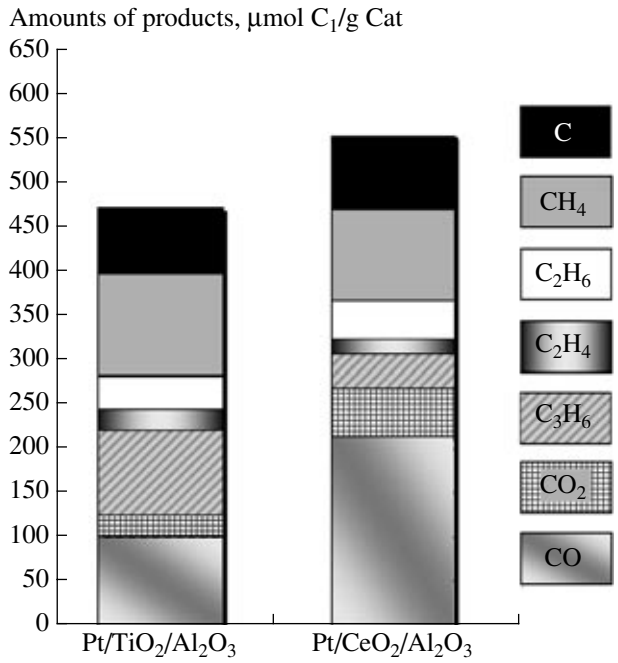

Fig. 3. Outcome of propane oxidation in the cyclic mode.

XPS

X-ray photoelectron spectra were recorded on an XSAM-800 spectrometer. The exciting radiation was AlK_α, with an energy of $h\nu$ = 1486.6 eV.

To take into account the differential charging effect, the positions of photoelectron lines in the spectra were determined relative to the Al2*p* line of the support (E_b = 74.5 eV). Catalyst samples were reduced in flowing argon containing 1% propane at 400°C for 20 min in a special-purpose reactor [11] attached to the spectrometer. The reduced samples were transferred to the spectrometer chamber in an airless atmosphere.

RESULTS AND DISCUSSION

Composition of the Product of Propane Oxidation in the Cyclic Mode

Figure 3 shows product composition data for propane oxidation on the Pt/TiO_2/Al_2O_3 and Pt/CeO_2/Al_2O_3 catalysts in a cycle including ten propane pulses. Clearly, as compared to the mixed-feedstock (steady-state) propane oxidation, the alternating-feed (cyclic) propane oxidation yields a quite different product: while the steady-state process results in deep propane

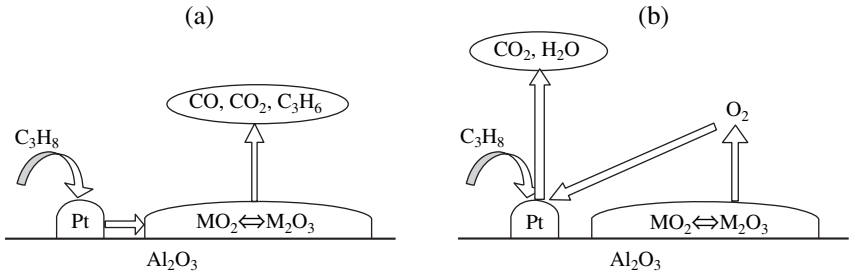

Fig. 4. Possible mechanisms of the reaction.

oxidation to CO_2 and H_2O, the cyclic process is characterized by a higher CO selectivity and apparently favors the oxidative dehydrogenation of hydrocarbons. Methane and ethane are present in the catalysate along with CO, CO_2, C_3H_6, and C_2H_4.

Note that the course of the process depends considerably on the oxygen-storing component of the catalytic system. $Pt/CeO_2/Al_2O_3$ affords more CO (221 μmol C_1/g Cat) than $Pt/TiO_2/Al_2O_3$ (99 μmol C_1/g Cat). However, the CO_2-containing catalyst produces more than twice as much CeO_2 as the TiO_2-containing catalyst. At the same time, $Pt/TiO_2/Al_2O_3$ affords more propylene (96 μmol C_1/g Cat) and ethylene (24 μmol C_1/g Cat). The methane and ethane contents of the catalysate after ten propane pulses are nearly the same for $Pt/TiO_2/Al_2O_3$ and $Pt/CeO_2/Al_2O_3$. The amount of condensation products is somewhat smaller for the $Pt/TiO_2/Al_2O_3$ catalyst.

Possible Process Mechanisms

The two most probable mechanisms of propane oxidation in the alternating-feed mode are depicted in Fig. 4.

In the first mechanism (Fig. 4a), C_3H_8 is activated on Pt and the activated species move to TiO_2 or CeO_2, where they are oxidized by chemically bound oxygen. A similar mechanism is considered for methane oxidation [9].

Periodic propane oxidation can also proceed through the desorption of stored oxygen from TiO_2 or CeO_2 into the gas phase (Fig. 4b) followed by a reaction between the hydrocarbon and desorbed oxygen. Considerable oxygen desorption was actually observed for V–Sb oxide catalysts [12]. In this mechanism, the process conditions are identical to those in the steady-state oxidation, in which propane and oxygen are simultaneously present in the gas phase. The contribution of the desorbed oxygen to the cyclic oxidation of propane was estimated by oxygen desorption measurements. The amount of oxygen leaving the catalyst surface at 400°C under the reaction conditions was estimated by the O_2 ID method. The total amount of desorbable oxygen was determined by the O_2 TPD method.

The O_2 ID data obtained at 400°C are presented in Fig. 5. Clearly, $Pt/TiO_2/Al_2O_3$ and $Pt/CeO_2/Al_2O_3$ desorb only a little oxygen over the initial ~120 s. It is significant that the Pt-free systems (TiO_2/Al_2O_3 and CeO_2/Al_2O_3) do not desorb any oxygen. The total amount of desorbed oxygen is 0.10 μmol O_2/g Cat for $Pt/TiO_2/Al_2O_3$ and 0.12 μmol O_2/g Cat for $Pt/CeO_2/Al_2O_3$.

The O_2 TPD spectra of $Pt/TiO_2/Al_2O_3$ and $Pt/CeO_2/Al_2O_3$ (Fig. 6) indicate two regions of oxygen desorption, namely, 100 and 480–620°C. The weak peak in the lower temperature region is due to the desorption of physically adsorbed oxygen. The amount of oxygen desorbed in this region is 0.40 and 0.60 μmol O_2/g Cat for $Pt/TiO_2/Al_2O_3$ and $Pt/CeO_2/Al_2O_3$, respectively. The amount of oxygen desorbed at 480–620° is 4.60 μmol O_2/g Cat for $Pt/TiO_2/Al_2O_3$ and 5.30 μmol O_2/g Cat for $Pt/CeO_2/Al_2O_3$. Comparing the data converted to 1 μmol of TiO_2 with earlier reported data [7] suggests that the amount of desorbed oxygen is very small as compared to the amount of oxygen reacting with propane:

Catalyst	Oxygen desorption		Stored oxygen [7]	
	μmol O_2/g Cat	μmol O_2/μmol TiO_2	derived from the chemical equation (I)*, μmol O_2/μmol TiO_2	derived from the chemical equation (II)**, μmol O_2/μmol TiO_2
1%Pt/10%TiO_2/Al_2O_3	4.60	0.002	0.185	0.056

* $C_3H_8 + 10O_{ox} = 3CO_2 + 4H_2O$ (I).
** $C_3H_8 + 3O_{ox} = 3CO + 4H_2$ (II).

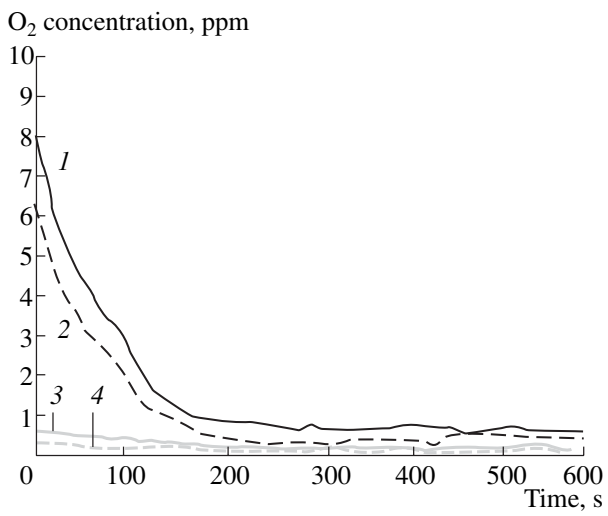

Fig. 5. Isothermal desorption of oxygen at 400°C from the catalysts (*1*) 1%Pt/10%CeO_2/Al_2O_3, (*2*) 1%Pt/10%CeO_2/Al_2O_3, (*3*) 10%CeO_2/Al_2O_3, and (*4*) 10%TiO_2/Al_2O_3.

Since the TPD peaks of the Pt/TiO_2/Al_2O_3 and Pt/CeO_2/Al_2O_3 systems appear in the same temperature region as the peaks characterizing the Pt/Al_2O_3 system, they can be assigned to oxygen desorbed from Pt. No O_2 desorption from Al_2O_3 was observed.

The O_2 ID and O_2 TPD data suggest that the oxygen desorbed from the catalyst surface into the gas phase contributes insignificantly to propane oxidation in the cyclic mode. It is also evident that the oxygen of TiO_2 and CeO_2 participates in the process. The reaction between C_3H_8 and the lattice oxygen of the catalyst must lead to changes in the oxidation state of Ti or Ce.

Our XPS data prove that the metals change their oxidation states. The spectra of the original and reduced catalysts are presented in Fig. 7. In order to separate the overlapping Ce lines, we deconvolved the spectra into doublets as a combination of two Gaussian–Lorentzian functions. Either component of the Ce3$d_{5/2}$–Ce3$d_{3/2}$ doublet consists of three Ce(IV) lines. By convention [13], they are designated v', v'', and v''' for the 3$d_{5/2}$ state and u', u'', and u''' for the 3$d_{3/2}$ state. The binding energies characterizing the 3$d_{5/2}$ state are 882.7, 889.0, and 898.6 eV and those characterizing the 3$d_{3/2}$ state are 901.1, 907.4, and 917.0 eV. The physical processes giving rise to these lines in the Ce3*d* spectrum are considered in detail elsewhere [14]. Quantitative analysis of the lines shown in Fig. 7 has demonstrated that the original catalyst contains a small amount (~13%) of Ce(III). The Ce3*d* lines characterizing Ce(III), designated v' and u', occur at 885.9 and 904.3 eV. Since the other two lines characterizing Ce(III) (v^0 and u^0) are much weaker than the v'/u' doublet [13], they were not involved in the deconvolution procedure.

It is evident from the spectra shown in Fig. 7 that treating the catalyst with C_3H_8 at 400°C strengthens the u' and v' lines markedly, indicating a buildup of Ce(III) ions in the surface layer. The proportion of Ce(III) increases to 28%. A similar situation is observed for cerium oxide reacting with SO_2 in the presence of oxygen [15]: the v' and u' lines grow markedly, while the lines due to Ce(IV) weaken noticeably.

Thus, O_2 ID and O_2 TPD data demonstrate that, under the reaction conditions examined, the desorption of oxygen from the catalyst surface into the gas phase is insignificant. Our XPS data prove that propane is oxidized by the lattice oxygen of the catalyst.

The Role of Platinum

Averaged product composition data for propane oxidation on the TiO_2- and CeO_2-containing catalysts in a cycle including ten propane pulses are listed in the table.

Clearly, platinum markedly increases the reaction rate. This makes it possible to carry out the reaction at much lower temperatures than in the case of CeO_2/Al_2O_3 or TiO_2/Al_2O_3, over which no significant C_3H_8 conversion is observed up to 550–600°C. The data available on cyclic methane oxidation [9, 16, 17] suggest that C–H and C–C bonds in propane molecules break on Pt to yield reactive intermediates, which are then oxidized by TiO_2 or CeO_2 lattice oxygen. The breaking of the C–C bonds is proved by the presence of

Product composition resulting from propane oxidation in the cyclic reactant supply mode*

Products	TiO_2/Al_2O_3	Pt/Al_2O_3 + TiO_2/Al_2O_3	Pt/TiO_2/Al_2O_3	Products	CeO_2/Al_2O_3	Pt/Al_2O_3 + CeO_2/Al_2O_3	Pt/CeO_2/Al_2O_3
CO	0	124	99	CO	0	118	221
CO_2	2	12	20	CO_2	3	18	53
C_3H_6	0	44	96	C_3H_6	0	71	39
C_2H_4	0	12	24	C_2H_4	0	14	16
C_2H_6	0	23	36	C_2H_6	0	19	43
CH_4	0	144	112	CH_4	0	153	103
C	0	126	73	C	0	114	82

* The amounts of products are in μmol C_1/g Cat.

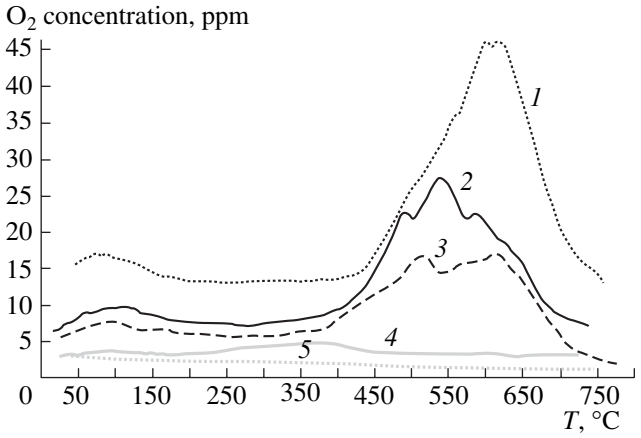

Fig. 6. Temperature-programmed desorption of oxygen from the catalysts (*1*) 1%Pt/Al_2O_3, (*2*) 1%$Pt/10\%CeO_2/Al_2O_3$, (*3*) 1%$Pt/10\%TiO_2/Al_2O_3$, (*4*) 10%CeO_2/Al_2O_3, and (*5*) 10%TiO_2/Al_2O_3.

methane and ethane in the reaction product. This bond breaking proceeds up to the formation of elementary carbon, which can be removed by oxidation to CO and CO_2 with an air pulse.

In the first possible mechanism of the reaction (Fig. 4a), the reactants (O_2 and/or C_3H_8) are activated on Pt and the activated species are transferred to TiO_2 or CeO_2, where they are oxidized by chemically bound oxygen. Here, the following question arises: How are the activated species transferred between Pt and TiO_2 or CeO_2? Most likely, they are transferred through the gas phase or by a spillover mechanism. In order to elucidate this point, we compared the catalytic properties of the supported catalysts $Pt/TiO_2/Al_2O_3$ and $Pt/CeO_2/Al_2O_3$ with those of the mechanical mixtures Pt/Al_2O_3 + TiO_2/Al_2O_3 and Pt/Al_2O_3 + CeO_2/Al_2O_3.

Comparison of the results obtained for the supported catalysts $Pt/TiO_2/Al_2O_3$ and $Pt/CeO_2/Al_2O_3$ and for the corresponding mechanical mixtures Pt/Al_2O_3 + TiO_2/Al_2O_3 and Pt/Al_2O_3 + CeO_2/Al_2O_3 (table) suggests that the reaction on these catalytic systems proceeds by similar mechanisms. The spillover of intermediates on the surface of the mechanical mixtures seems to be unlikely because of the long distance between the promoting component (Pt) and the oxidizing component (TiO_2 or CeO_2). Therefore, part of the intermediates are assumed to be transferred through the gas phase.

However, the products obtained with the mechanical mixtures and with the supported catalysts (whose components are close to each other) have somewhat different compositions. For example, $Pt/CeO_2/Al_2O_3$ affords much more carbon monoxide (221 μmol C_1/g Cat) than Pt/Al_2O_3 + CeO_2/Al_2O_3 (118 μmol C_1/g Cat). Among the TiO_2-containing systems, the Pt/Al_2O_3 + TiO_2/Al_2O_3 mixture affords the highest CO yield. Employing the supported system $Pt/TiO_2/Al_2O_3$ allows the propylene and ethylene yields to be considerably increased (table).

Furthermore, $Pt/TiO_2/Al_2O_3$ and $Pt/CeO_2/Al_2O_3$, as compared to the corresponding mechanical mixtures, are less prone to carburization and yield smaller amounts of propane cracking products.

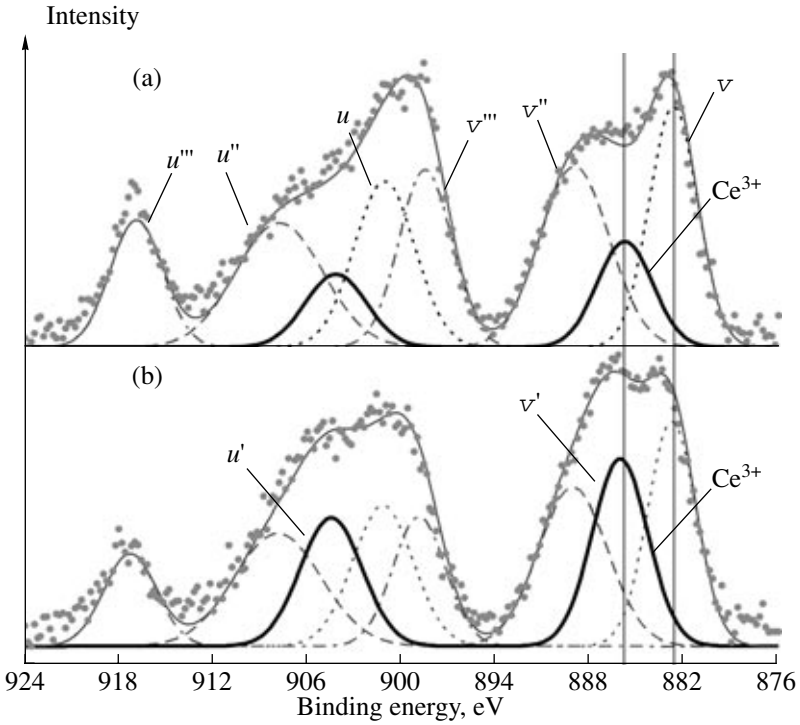

Fig. 7. X-ray photoelectron spectra of (a) original 1%$Pt/10\%CeO_2/Al_2O_3$ and (b) the same sample reduced with C_3H_8 at 400°C.

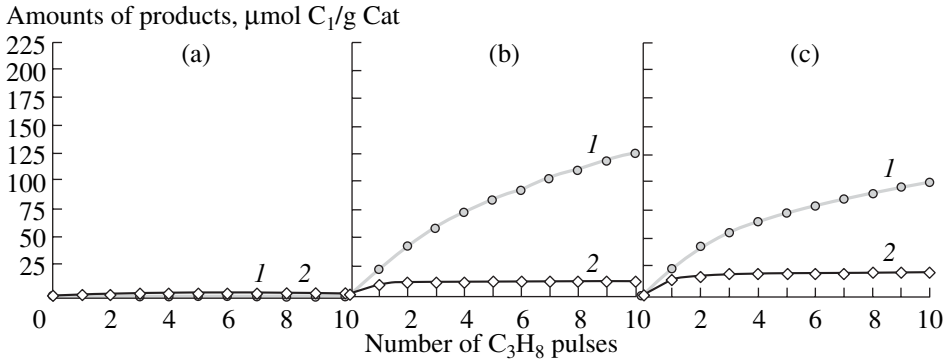

Fig. 8. Amounts of (*1*) CO and (*2*) CO_2 as a function of the number of propane pulses fed to the catalyst: (a) 10% TiO_2/Al_2O_3, (b) 1% Pt/Al_2O_3 + 10% TiO_2/Al_2O_3, and (c) 1% Pt/10% TiO_2/Al_2O_3.

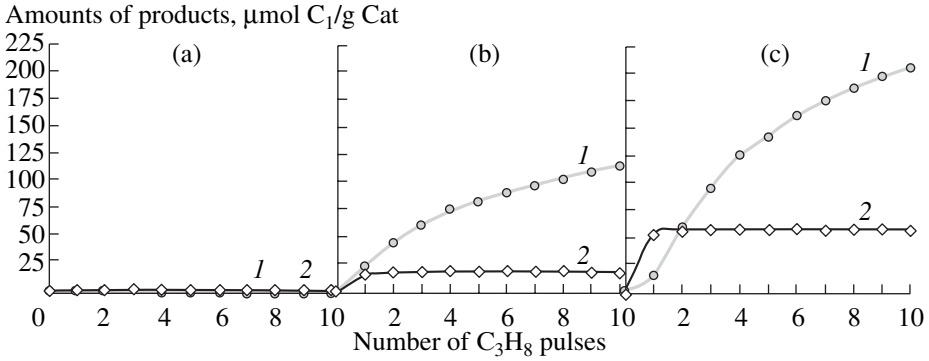

Fig. 9. Amounts of (*1*) CO and (*2*) CO_2 as a function of the number of propane pulses fed to the catalyst: (a) 10% CeO_2/Al_2O_3, (b) 1% Pt/Al_2O_3 + 10% CeO_2/Al_2O_3, and (c) 1% Pt/10% CeO_2/Al_2O_3.

The above facts suggest that, along with the transfer of intermediates from Pt to TiO_2 or CeO_2 through the gas phase, the spillover of intermediates on the catalyst surface also makes some contribution to propane oxidation.

Figures 8 and 9 show how the amounts of CO and CO_2 converted to one carbon atom (μmol C_1/g Cat) increase as a function of the number of propane pulses for the TiO_2- and CeO_2-containing systems, respectively.

The supported catalyst $Pt/TiO_2/Al_2O_3$ and the mechanical mixture Pt/Al_2O_3 + TiO_2/Al_2O_3 are similar (Fig. 8), with the only difference being that the reaction over $Pt/TiO_2/Al_2O_3$ yields a smaller amount of CO and a larger amount of CO_2.

The reaction over $Pt/CeO_2/Al_2O_3$ yields more CO_2 than the reaction over Pt/Al_2O_3 + CeO_2/Al_2O_3. Therefore, there is a spillover of intermediates on the catalyst surface.

CONCLUSIONS

This study has demonstrated that propane oxidation in the cyclic, catalyst oxidation–reduction mode, as compared to steady-state propane oxidation, shows a much lower selectivity toward complete oxidation products and a higher selectivity toward partial oxidation products.

The composition of the oxidation product depends strongly on the nature of the oxygen-storing component (TiO_2 or CeO_2). With the $Pt/CeO_2/Al_2O_3$ catalyst, the main oxidation product is carbon monoxide. The $Pt/TiO_2/Al_2O_3$ catalyst yields considerable amounts of propylene and ethylene.

The O_2 ID and O_2 TPD data suggest that the oxygen desorbed from the catalyst surface into the gas phase makes only a negligible contribution to propane oxidation. The XPS data prove that propane is oxidized by the chemically bound oxygen of the catalyst.

The presence of platinum is a necessary condition for the process to take place at low temperatures.

The following oxidation mechanism follows from the above results: propane is activated on Pt, and the activated species move to the oxygen-storing component through the gas phase or another way. The intermediates are oxidized by the chemically bound oxygen of TiO_2 or CeO_2.

REFERENCES

1. Cavani, F. and Trifiro, F., *Catal. Today*, 1999, vol. 51, p. 561.
2. Satterfield, Ch., *Heterogeneous Catalysis in Practice*, New York: McGraw-Hill, 1980.
3. Arutyunov, V.S. and Krylov, O.V., *Okislitel'nye prevrashcheniya metana* (Oxidative Conversions of Methane), Moscow: Nauka, 1998.
4. Ballarini, N., Cavani, F., Ferrari, M., Catani, R., and Cornaro, U., *J. Catal.*, 2003, vol. 213, p. 95.
5. Contractor, R.M., Bergna, H.E., Horowitz, H.S., Blackstone, C.M., Malone, B., Torardi, C.C., Griffiths, B., Chowdhry, U., and Sleight, A.W., *Catal. Today*, 1987, vol. 1, nos. 1–2, p. 49.
6. Rosso, R.Del., Kaddouri, A., Mazzocchia, C., Gronchi, P., and Centola, P., *Catal. Lett.*, 2000, vol. 69, p. 71.
7. Sinel'nikov, V.V., Tolkachev, N.N., and Stakheev, A.Yu., *Kinet. Katal.*, 2005, vol. 46, no. 4, p. 585.
8. Kaspar, J., Fornasiero, P., and Hickey, N., *Catal. Today*, 2003, vol. 77, p. 419.
9. Bychkov, V.Yu., Sinev, M.Yu., Korchak, V.N., Aptekar, E.L., and Krylov, O.V., *Kinet. Katal.*, 1986, vol. 27, no. 5, p. 1190.
10. Pantu, P., Kim, K., and Gavalas, G.R., *Appl. Catal., A*, 2000, vol. 193, p. 203.
11. German Patent 289596, 1991.
12. Bychkov, V.Yu., Sinev, M.Yu., and Vislovskii, V.P., *Kinet. Katal.*, 2001, vol. 42, no. 4, p. 632.
13. Romeo, M., Bak, K., El Fallah, J., Le Normand, F., and Hilaire, L., *Surf. Interface Anal.*, 1993, vol. 20, p. 508.
14. Fujimori, A., *J. Magn. Magn. Mater.*, 1985, vols. 47–48, p. 243.
15. Smirnov, M.Yu., Kalinkin, A.V., Pashis, A.V., Sorokin, A.M., Noskov, A.S., Bukhtiyarov, V.I., Kharas, K.S., and Rodkin, M.A., *Kinet. Katal.*, 2003, vol. 44, no. 4, p. 629.
16. Denton, P., Odier, E., and Mirodatos, C., *Stud. Surf. Sci. Catal.*, 2001, vol. 138, p. 13.
17. Sadykov, V.A., Kuznetsova, T.G., Veniaminov, S.A., *et al.*, *React. Kinet. Catal. Lett.*, 2002, vol. 76, no. 1, p. 83.